International Journal of Thermophysics, Vol. 22, No. 4, 2001

In situ X-ray Diffraction Studies of a Multilayered Membrane Fluid under Confinement and Shear[1]

Y. Li,[2,3] Y. Golan,[4,5] A. Martin-Herranz,[6] O. Pelletier,[2] M. Yasa,[2] J. N. Israelachivili,[4] and C. R. Safinya[2]

The structure of a fluid membrane system composed of surfactant-co-surfactant-oil-water mixtures has been investigated under confinement and shear conditions. Small angle x-ray scattering (SAXS) was employed with a second generation x-ray surface forces apparatus (XSFA-II) to study the time evolution of the orientational structure of the lamellar fluid under oscillatory shear. In a regime of relatively big confinement gap ($\sim 800\,\mu$m) and small shear amplitude ($\sim 40\,\mu$m), direct evidence of an "orientational phase separation" behavior, where a surface boundary layer adopts different orientation and separates from the bulk region, was observed for the first time. Under continuous shearing, the surface boundary layer grows in thickness and aligns towards a shear-favored (low friction) state while the bulk orientation remains unchanged. To further investigate the effects of surface confinement, we spatially mapped, in $\sim 1\,\mu$m sections, the orientation structure of the lamellar fluid sample confined between two glass surfaces using a micro-focused x-ray beam produced by a linear Bragg–Fresnel lens at the Advanced Photon Source. The data confirmed the expected trend that the smectic domains align progressively better with respect to the surface as they approach the surface.

KEY WORDS: complex fluids; confinement; surface forces; x-ray micro-diffraction.

[1] Paper presented at the Fourteenth Symposium on Thermophysical Properties, June 25–30, 2000, Boulder, Colorado, U.S.A.

[2] Materials Research Laboratory, Materials Department and Physics Department, University of California at Santa Barbara, Santa Barbara, California 93106, U.S.A.

[3] To whom correspondence should be addressed. E-mail: youli@mrl.ucsb.edu

[4] Materials Research Laboratory, Materials Department and Chemical Engineering Department, University of California at Santa Barbara, Santa Barbara, California 93106, U.S.A.

[5] Present address: Department of Materials Engineering, Ben-Gurion University of the Negev, Beer-Sheva 84105, Israel.

[6] Present address: Unilever Research Port Sunlight Lab, Wirral CH63 3JW, Merseyside, United Kingdom.

0195-928X/01/0700-1175$19.50/0

1. INTRODUCTION

The structure of complex fluids under confinement and shear has been studied extensively in the last twenty years. These studies have fundamental aspects in, e.g., correlating lateral force features with structural transitions, as well as practical implications such as designing novel lubricants based on structured molecular fluids. The visco-elastic properties of these structured fluids were found to be highly dependent on the molecular orientation. In fluids where the molecules are either arranged in layers (smectic or lamellar phase) or as hexagonal arrays of cylindrical micelles, very low frictional forces were measured [1]. This has been attributed to molecules realigning under shear to low frictional states, such as the "sliding layer" arrangement in the lamellar phase and the "rolling cyllinder" arrangement in the hexagonal phase. The development of techniques that can directly probe structural and chemical evolution in shearing contacts at real-time is essential for understanding this and other complicated tribological processes. Earlier work using a x-ray Couette shear cell has shed some light on the structure of bulk molecular fluids under shear [2, 3]. For measurements of confined thin films, the x-ray surface forces apparatus (XSFA) [4, 5], adapted directly from the SFA-III surface forces apparatus [6], is an ideal tool because of its capability to measure structural changes in the sample upon shear at well-defined gap separations.

Recent developments have led to the second generation x-ray surface forces apparatus (XSFA-II), with normal and shear force measurement capabilities coupled with *in-situ* small angle x-ray scattering experiments under static confinement and oscillatory shear conditions in a well-defined environment. The results of the first study using the XSFA-II of the dynamical evolution of the orientational structure of a four-component lyotropic membrane fluid system under shear are presented here. In these experiments the x-rays impinge on the sample in the direction normal to the confining surfaces, therefore giving orientation information about the lamellar domains normal to the surfaces.

Using a micro-focused x-ray beam in the glancing incidence geometry, measurements were made on the same sample system confined between glass surfaces in a rectangular capillary. These measurements are complementary to the XSFA studies and provide the orientation structure of the smectic layers parallel to the confining surfaces. More importantly, the $\sim 1\ \mu$m size focused beam, which was produced using a Bragg–Fresnel lens at the Advanced Photon Source, a third generation synchrotron, enabled us to spatially map the orientational profile of the sample in thin (comparable to beam size) sections. This makes possible the visualization of surface effects on domain orientations as a function of the distance from the surface.

2. MATERIALS

The samples we studied consisted of mixtures of sodium dodecyl sulfate (SDS, surfactant), pentanol (co-surfactant), dodecane (oil) and water. This system has a well-characterized, rich phase diagram [7], which allows us to access a variety of molecular structures by changing the composition. For the experiments described here, we focused on samples in the L_α (lamellar) phase. In this phase region, because the molecules are arranged in stacked layers which are intrinsically anisotropic, the application of confining surfaces or external shear is expected to induce rearrangement of domains into energetically favorable (low friction) structures.

3. RESULTS FROM XSFA-II STUDIES

The second generation x-ray surface forces apparatus (XSFA-II) is schematically illustrated in Fig. 1. The completely redesigned sealed sample chamber has three windows to allow simultaneous coaxial optical and x-ray measurements. Incident and scattered x-rays are transmitted through an ultrathin (50 μm) silica front window and a beryllium back window, both of which have low x-ray absorption. The visible light signal is separated from the x-rays by a mirror and passed through a photo-spectrometer for monitoring the gap using FECO fringes (gap size down to angstrom level has been achieved). A side port allows direct sample injection in between the two confining surfaces from outside of the sample chamber. Humidity control is achieved by using a reservoir feedthrough on the housing. The surfaces are made of quartz-backed mica mounted on

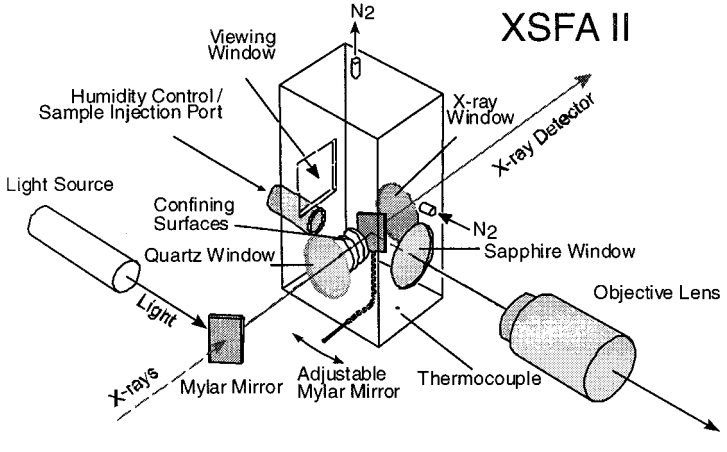

Fig. 1. Schematic diagram of the XSFA-II.

curved aluminum disks [8]. Temperature and humidity sensors can be incorporated into the housing. A friction device attached to the front side of the apparatus measures the frictional force between the two surfaces in tandem with optical and x-ray measurements.

The experiments were carried out using an 18 kW Rigaku rotating anode x-ray source ($\lambda = 1.54$ Å) and a small angle x-ray spectrometer with a 2-D image plate detector. The beam size on the sample was 0.5 mm × 0.5 mm. We had chosen to study the behavior of these lamellar fluid samples in fairly large gaps ($\sim 800\,\mu$m) in order to maximize x-ray scattering signal. Two x-ray diffraction patterns from a lamellar fluid sample under static and shear conditions are shown in Fig. 2. The ring of scattering intensity corresponds to the first-order (001) peak of the smectic layer spacing. A uniform ring would suggest isotropically distributed membrane domains. Clearly, even when the sample was initially injected in between the surfaces (static data), the surface confinement effects were already aligning the smectic domains in preferred orientations, which varied between different fillings of the sample. The direction where the scattering is strongest indicates the preferred orientation (indicated by the lines in the images) of the plane normal to the smectic layers. Figure 2c illustrates the three possible real space orientations, labeled "a," "b," "c" of the smectic layers with respect to shear. In the data shown in Fig. 2a (no shear), the surfaces are oriented parallel to the plane of the image, and the preferred orientation is close to the "b" orientation at $\varphi = 0$, which is the direction of shear. The "b" orientation is a high friction state and is generally forbidden at high shear rates [2].

The shear is applied by moving one of the surfaces in the XSFA-II relative to another using a piezoelectric transducer. Because of the limited amplitude in the movement ($\sim 40\,\mu$m for the experiments) and the large

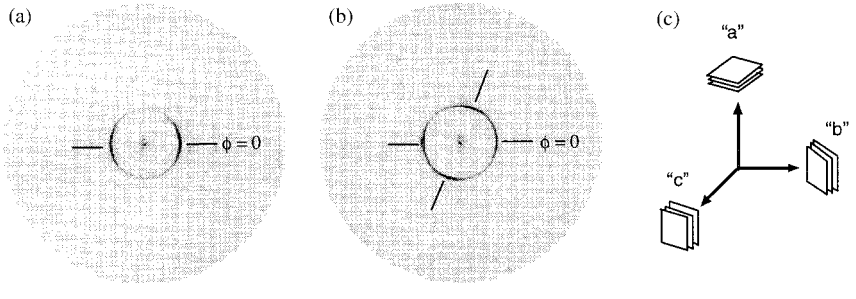

Fig. 2. X-ray diffraction patterns collected using the XSFA-II from an SDS lamellar sample (a, b). Data shown in (a) were taken at static (no shear) condition, whereas (b) shows the 2-D diffraction data of the same sample after 15 h of shear. The three possible real space orientations of the lamellar layer with respect to the shear surface are defined in (c).

gap size used, the effective shear rate is small. In fact, this shear rate is below what most people have studied before. What is interesting and somewhat surprising is that the sample *did* respond to this perturbational shearing, albeit on a much slower time scale. Figure 2b shows the diffraction pattern from the same sample as in Fig. 2a, but after 15 h of oscillatory shearing (frequency = 1 Hz). The data show two populations of the aligned smectic planes, almost orthogonal to each other. Because the data are on the same intensity scale, Fig. 2b strongly suggests that the initial "b" oriented domains have been redistributed into a combination of "b" and "a" oriented domains. The transition from "b" to "a" orientation makes sense because the "a" orientation is less shear-resistant. Contrary to high shear rate experiments on bulk samples [2], the "b" orientation did not vanish and is therefore not forbidden at this low shear rate (although it's clearly not favored).

Fortuitously, the long time scale of the orientation transition provided us with the opportunity to study the dynamic behavior of the transition.

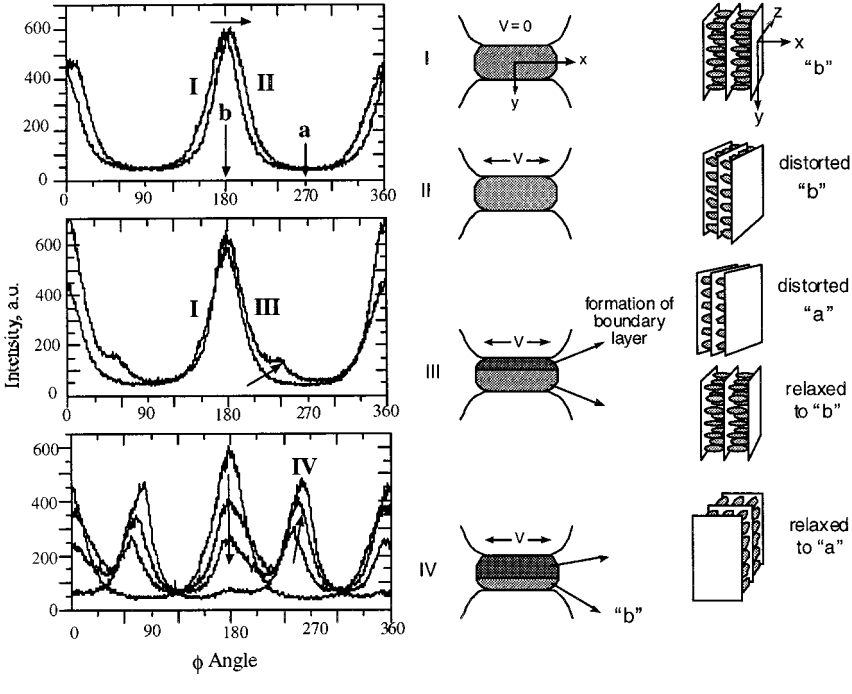

Fig. 3. Time resolved SAXS data showing evolution of the domain orientations (left) and schematic representation of the "orientational phase separation" model (right). See text for details.

X-ray diffraction data taken every half-hour after the onset of shear gave a clear evolutionary picture of the process. In Fig. 3 (left) we show the result of such a time series. The plots are x-ray intensities as a function of the in-plane φ angle on the ring of the diffraction peak. On a short time scale (<1 h after the onset of shear) (top graph), the intensity maximum (**I**) (the orientation of the domains) shifts slightly towards a larger angle (**II**), which is consistent with the shear-resistant "b" oriented domains being strained by the shear field and tilting towards the "a" orientation. At some point (1 to 2 h), a distinct second peak occurs in the diffraction pattern (curve **III** in middle graph, diagonal arrow), indicating a different domain orientation. It's important to note that the first peak ("b" domains) at this point relaxes back to the original angular position. *We interpret this result as the rupture of the film into two layers: one bulk layer maintaining the initial orientation and the other boundary layer induced by shear* (see Fig. 3, right graph **III** for a schematic representation). From there on, the second diffraction peak increases in intensity over time with shear and shifts continuously towards the shear-favored "a" orientation, while the original "b"-oriented peak decreases in intensity correspondingly. This suggests that under continuous shear the boundary layer not only aligns towards the low-friction "a" orientation, but also grows in thickness. This scenario is depicted in graph **IV** in Fig. 3 (right). To our knowledge this is the first experimental observation of such "orientational phase separation" behavior.

The assumption that the surface layer originates from the moving surface is not unreasonable based on the fact that the local shear force is highest at the surface-sample interface. Although the shear amplitude is small compared to the overall gap size, the shear force in the local surface layer apparently was high enough to induce orientation transitions towards the low-friction state. After the separation of the surface layer from the bulk, the shearing force continues to be transmitted to the bulk sample. This explains the gradual propagation over time of the surface layer front into the bulk region. Asymptotically, one expects that the surface layer would occupy the entire gap. The long time scale of this process is a direct consequence of the small shear amplitude. Therefore, this low shear rate case might be considered as a "slow motion" glimpse of what might happen quickly at high shear rates, such as that in the x-ray Couette shear cell where all smectic domains adopt the low friction "a" orientation in a short time [2]. It is likely that the viscosity of the sample had some effects on the formation and propagation of the surface layer. This will be investigated in future experiments by varying the concentration of the membrane in the fluid phase.

4. RESULTS FROM X-RAY MICRO-DIFFRACTION

Recent advances in x-ray micro-focusing optics have made available submicron size intense x-ray beams at third generation synchrotron sources, which greatly enhanced the capabilities of hard x-ray microscopy and micro-diffraction methods [9, 10]. These microbeams are ideally suited for studying materials under confinement because the microscopic beam size permits spatially resolved structural measurement in the area of interest, e.g., in the confinement gap.

We used a line-focused beam produced using a linear Bragg–Fresnel lens (BFL) at the Advanced Photon Source to map the orientation profile of the lamellar domains in the SDS sample confined in a rectangular capillary. The diffractive x-ray micro-lenses, developed by us at UCSB, were fabricated by depositing Au (thickness ~ 2000 Å, roughly corresponding to a π phase shift compared to air) in Fresnel zones patterned by electron beam lithography on a (111) Si substrate. This is a much simpler process than the traditional BFL fabrication process based on reactive ion etching methods [9, 10]. The optical properties of these novel metal-layer Bragg–Fresnel lenses, which were characterized at the APS before the micro-diffraction experiments, will be described elsewhere.

The micro-diffraction setup is shown schematically in Fig. 6, with an optical micrograph of the beam condensing linear BFL. The vertical focusing BFL produced a $1\,\mu$m (vertical) $\times 50\,\mu$m (horizontal) beam at the sample position. The focal spot size was determined by source demagnification, the actual diffraction-limited resolution of the lens is $\sim 0.3\,\mu$m. Because the confinement occurred only in the vertical direction, it was advantageous to use an unfocused horizontal beam to integrate over a larger sample area

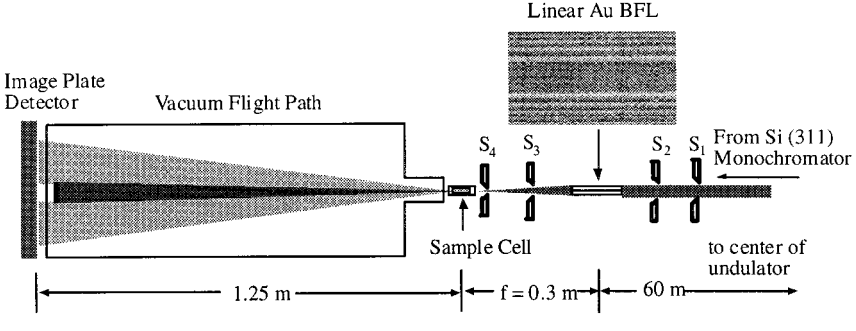

Fig. 4. Illustration of micro-diffraction set up using a linear Bragg–Fresnel lens (BFL) at Beamline 2-ID-C at the Advanced Photon Source. Insert: an optical micrograph of the linear BFL used in the experiments (only central zones are shown). The diffraction limited resolution of the lens was $\sim 0.3\,\mu$m (lens aperture = 0.1 mm (v) $\times$ 10 mm (h)).

for enhanced signal. The extensive use of x-ray slits ($S_1 - S_4$) upstream of the sample and an evacuated 1.25-m flight path after the sample reduces background scattering in the small angle region ($q_{min} \sim 0.01$), where the smectic layering peaks occur.

The gap size in the rectangular capillaries ranged from 20 to 100 μm. The microbeam was positioned at the desired sample region based on x-ray tranmission images of the sample cell, which were cellected by scanning the capillary through the x-ray beam. Using this method, we were able to collect x-ray diffraction focused at well defined positions in the sample volume, with a spatial resolution of the order of a micron, to investigate the structural variations as a function of the distance from the confining surface. In Fig. 5, we present x-ray diffraction data (recorded on an image plate detector) from two sections of the SDS sample. The diffraction pattern on the left was taken from the sample near the center of the capillary while the image on the right corresponds to a 1 μm section of the sample on the inner surface of the top capillary wall. Clearly, the smectic layers in both sections were strongly aligned parallel to the confining surfaces (the "c" orientation as shown in Fig. 2). However, it can be seen that the sample was better aligned (peaks sharper) near the surface than in the center. This is confirmed by plotting the x-ray intensity on the diffraction ring, as shown in Fig. 6, which depicts five in-plane φ-scans corresponding to diffraction data taken at 10 μm intervals starting from the surface. The data reveal a clear sharpening of the orientation peak (better alignment) going from the center towards the edge of the capillary. This is consistent with the expectation that the surface alignment effect becomes stronger

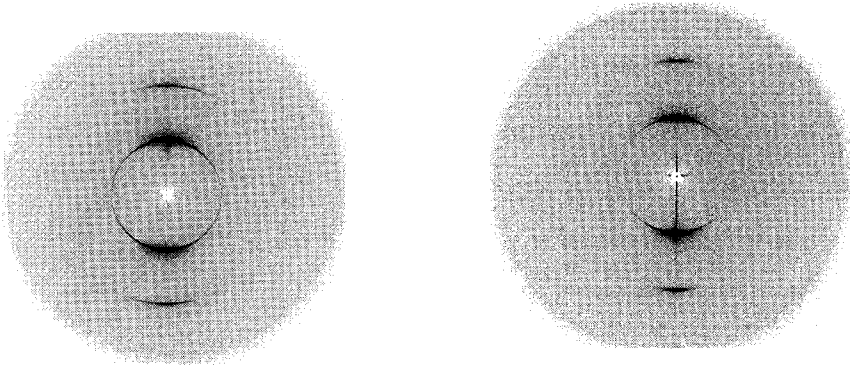

Fig. 5. Diffraction data (image plate) of the SDS sample at two positions in the capillary. The pattern on the left corresponds to the sample near the center of the capillary whereas the pattern on the right corresponds to the sample near the surface. The vertical streak of intensity seen on the image on the right is an artifact caused by residual slits scattering.

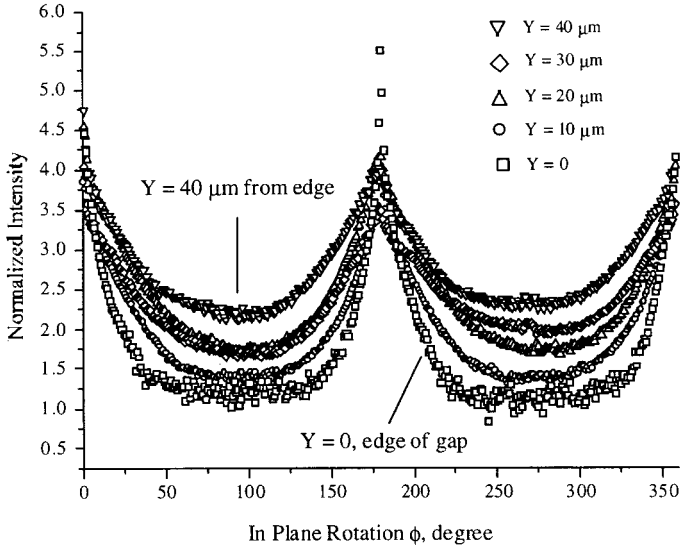

Fig. 6. In plane intensity profiles of SDS lamellar fluid mapped at five different positions in the confinement gap. The surface (inner wall of capillary) is at $y = 0$.

closer to the surface. This preliminary experiment opens up the possibility of combining the x-ray microprobe with the XSFA to further investigate the structural changes induced by shear. This new capability will provide the unambiguous experimental evidence for the surface layer formation and growth model discussed earlier.

5. CONCLUSION

We studied the confinement- and shear-induced structural changes in an SDS surfactant lamellar fluid using a second generation x-ray surface forces apparatus (XSFA-II) and x-ray micro-diffraction methods. At low shear rate, we observed the separation and growth of a surface layer from the bulk sample. Using a 1 μm x-ray microprobe, we mapped in micron-size sections the orientational distribution of the SDS sample confined in a flat x-ray capillary and showed that the smectic layers were better aligned near the surface than in the center of the capillary.

ACKNOWLEDGMENTS

This work was supported by ONR N00014-00-1-0214, NSF DMR-0076357 & DMR-9972246, the UC/Los Alamos Research (CULAR)

Program (STB-UC: 99-216), and University of California UC-Biotech Program (99-14). J. Israelachivili and Y. Golan wish to thank US-Israel Binational Science Foundation for Grant No. 9800395. This work made use of MRL Central Facilities supported by the National Science Foundation under award No. DMR00-80034. Use of the APS was supported by U.S. Department of Energy, Basic Energy Sciences, Office of Energy Research, under Contract No. W-31-109-Eng-38.

REFERENCES

1. C. R. Safinya and T. Fischer, to be published.
2. C. R. Safinya, E. B. Sirota, R. F. Bruinsma, C. Jeppesen, R. J. Piano, and L. J. Wenzel, *Science* **261**:588 (1993).
3. C. R. Safinya, E. B. Sirota, and R. J. Plano, *Phys. Rev. Lett.* **66**:1986 (1991).
4. S. H. J. Idziak, C. R. Safinya, R. S. Hill, K. E. Kraiser, M. Ruths, H. E. Warriner, S. Steinberg, K. S. Liang, and J. N. Israelachvili, *Science* **264**:1915 (1994).
5. S. H. J. Idziak, I. Koltover, J. N. Israelachvili, and C. R. Safinya, *Phys. Rev. Lett.* **76**:1477 (1996).
6. J. N. Israelachvili and P. M. McGuiggan, *J. Mat. Res.* **5**:2223 (1990).
7. G. S. Smith, E. B. Sirota, C. R. Safinya, R. J. Plano, and N. A. Clark, *J. Chem. Phys.* **92**:4519 (1990).
8. I. Koltover, S. H. J. Idziak, P. Davidson, Y. Li, C. R. Safinya, M. Ruths, S. Steinberg, and J. N. Israelachvili, *J. Phys. II France* **6**:893 (1996).
9. A. Snigirev, *Rev. Sci. Instr.* **66**:2053 (1995).
10. Y. Li, G. C. L. Wong, C. R. Safinya, E. Caine, E. L. Hu, D. Haeffner, P. Fernandez, and W. Yun, *Rev. Sci. Instr.* **69**:2844 (1998).